

## Analysis of thermal management in prismatic and cylindrical lithium-ion batteries with mass flow rate and geometry of cooling plate channel variation for cooling system based on computational fluid dynamics

Thalita Maysha Herninda<sup>a</sup>, Laurien Merinda<sup>a</sup>, Ghina Kifayah Putri<sup>a</sup>, Enda Grimonia<sup>a</sup>,  
Nur Laila Hamidah<sup>a\*</sup>, Gunawan Nugroho<sup>a</sup>, Erkata Yandri<sup>b</sup>, Ivar Zekker<sup>c</sup>, Idrees Khan<sup>d</sup>,  
Luqman Ali Shah<sup>e</sup> and Roy Hendroko Setyobudi<sup>b</sup>

<sup>a</sup> Department of Engineering Physics, Institut Teknologi Sepuluh Nopember (ITS) Surabaya, Gedung C dan E, Kampus ITS, Sukolilo Surabaya 60111, Indonesia

<sup>b</sup> Graduate School of Renewable Energy, Darma Persada University, Radin Inten 2, Pondok Kelapa, East Jakarta 13450, Indonesia

<sup>c</sup> Institute of Chemistry, University of Tartu, Ravila 14a, 50411 Tartu, Estonia

<sup>d</sup> Department of Chemistry, Bacha Khan University, Khyber Pakhtunkhwa 24420, Pakistan

<sup>e</sup> National Center of Excellence in Physical Chemistry (NCE), University of Peshawar, Pakistan

Received 24 September 2021, accepted 29 November 2021, available online 22 August 2022

© 2022 Authors. This is an Open Access article distributed under the terms and conditions of the Creative Commons Attribution 4.0 International License CC BY 4.0 (<http://creativecommons.org/licenses/by/4.0>).

**Abstract.** There is a global need for lithium-ion battery (LIB) with high specific power density and energy density; however, LIB is very sensitive to temperature. To guarantee the safety and performance of LIB, mini channel liquid-cooled plate was applied as a part of battery thermal management system. In this research, the effect of water mass flow rate and the geometry of liquid-cooled plate channel were investigated. The variation of geometry is affected by the width of the channel on the prismatic battery and the number of channels on the cylindrical battery. The results show that the battery temperature decreases with increasing the inlet mass flow rate, the number and width of cooling channels. Controlling the inlet mass flow rate and cooling channels is not necessary in case certain critical values are avoided. Thus, applying  $10^{-3}$  kg/s<sup>-1</sup> of mass flow rate in 8 mm channel width effectively decreased the prismatic battery temperature from 45 °C to 30 °C. Moreover, the use of wider channel decreases the pressure drop inside the channel. It can be concluded that by using eight cooling channels with 0.001 kg/s<sup>-1</sup> inlet mass flow rate, the maximum temperature can be controlled up to 12.06 °C for a cylindrical battery. This study helps increasing energy efficiency, which further promotes the circular economy program.

**Keywords:** battery thermal management system, circular economic program, electric vehicles, energy efficiency, green energy vehicles, mini channel cold plate.

### 1. INTRODUCTION

The growing concerns for energy scarcity derived from global warming and pollution encourage companies engaged in car manufacturing to create green energy vehicles [1]. Pure electric vehicles (EVs) and hybrid electric

vehicles (HEVs) are among the types of electric vehicles that are still under development [2]. EVs and HEVs are highly energy-efficient, less noisy and environmentally more sustainable than conventional vehicles [3]. Battery power plays a key role in the development of EVs. In order to create an electric vehicle that has a high efficiency, a battery with high specific power density and energy density is needed. Compared to other types of secondary

\* Corresponding author, [nurlaila.hamidah88@gmail.com](mailto:nurlaila.hamidah88@gmail.com)

batteries, lithium-ion battery (LIB) has the best performance when used for energy storage in electric vehicle. It has 500 to 1000 life cycles, no memory effect, low self-discharge rate and fast acceleration capability [4–6]. Despite many advantages, LIB is very sensitive to temperature [7]; at low temperatures LIB has poor performance and its electrode will degrade at high temperature [8]. During charge and discharge processes, a large amount of heat is generated due to electrochemical reactions, and resistance will further increase the battery temperature [9]. Thus, the battery must not be overcharged, as it will generate irreversible chemical reactions, which cause non-functional battery cells or decrease the performance and energy storage capacity. Therefore, battery thermal management system is absolutely necessary to maintain the performance of LIB.

Battery thermal management systems can be divided into three types depending on the cooling medium, i.e. air-based cooling, water-based cooling and phase change material (PCM). Generally, for LIB the most commonly used is air-cooled system, but it does not work in some conditions, such as fast charging and discharging conditions [10]. A comparative study on cooling methods for LIB [11] exploring various systems with different mediums found that the cooling system with liquid medium has the most effective thermal performance as it lowered the temperature by 14 °C. Furthermore, the results suggested that the liquid cooling system reduces temperature more than air cooling system and PCM cooling system due to a higher heat transfer coefficient. Thus, the liquid-based cooling system is a promising method for thermal management system in LIB [12]. In addition, research on the design of mini channel cold plate for liquid medium cooling system showed that the maximum battery temperature would decrease along with increasing the number of channels and inlet fluid flow rate [13]. The influence

of channel geometry has also been an important factor in the uniformity of the temperature in the battery and the pressure drop of the fluid.

Accordingly, a mini channel liquid-cooled cylinder plate is applied to prismatic and cylindrical LIB and the geometry of cooling channel and inlet mass flow rate related to the heat transfer theory are investigated. The aims of this research are to provide an effective cooling method and to develop guidelines for the thermal management system design for LIB.

## 2. METHODOLOGY

### 2.1. Physical problem

#### 2.1.1. Prismatic lithium-ion battery

A prismatic battery cell has dimensions of 118 × 63 × 10 mm. Aluminum plate with a thickness of 1 mm is placed on the side of lithium-ion battery at the inlet and outlet on both sides. Cooling fluid flows into the cold plate through the inlet and then splits into five directions, the geometric details are shown in Fig. 1. The LiCoO<sub>2</sub> type LIB is implemented while water is used as cooling fluid by varying the inlet mass flow rate and the width of channel and aluminum is used as cold plate. The specifications of battery, water, and aluminum plate are listed in Table 1.

The heat generated by the battery comes from the electrochemical reaction ( $Q_r$ ) and Joule heating ( $Q_j$ ). The heat generated from the electrochemical reaction can be calculated by Eq. 1:

$$Q_r = T\Delta S \frac{1}{nF}, \quad (1)$$

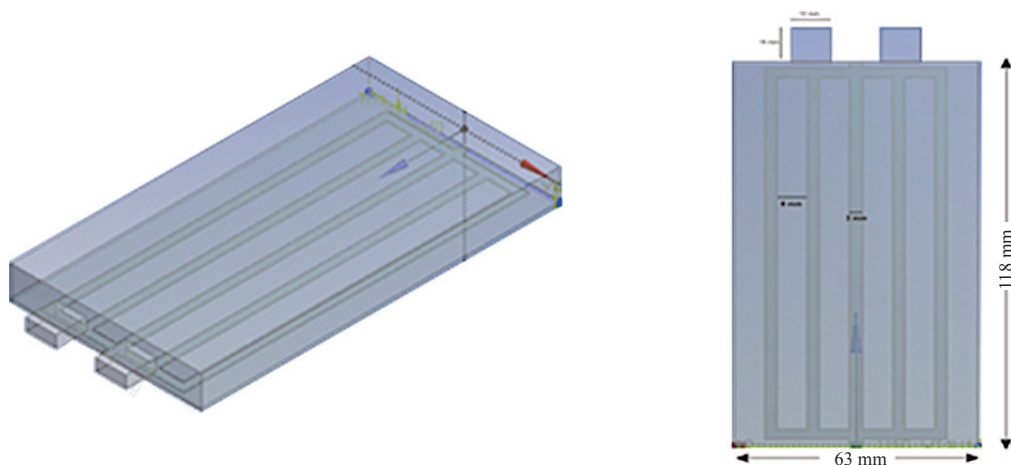


Fig. 1. Cell battery geometry and cold plate.

**Table 1.** Battery, aluminum, and water thermo-physical parameters

Material	$\rho$ (kg/m <sup>3</sup> )	$c_p$ (J/kg <sup>-1</sup> K <sup>-1</sup> )	$k$ (W/mK <sup>-1</sup> )
Aluminum	2719	817	202.4
Water	998.2	4128	0.6
Batteries	2500	1000	3

where  $T$  represents the operational temperature (°C) of the battery,  $\Delta S$  denotes entropy change (J mol<sup>-1</sup> K<sup>-1</sup>),  $F$  is Faraday constant (C·mol<sup>-1</sup>), and  $n$  is the number of electrons transferred. The main cause of Joule heating is the transfer of current within the internal resistance given by Eq. 2

$$Q_j = I(E - V), \tag{2}$$

where  $E$  and  $V$  are operating cell voltage (V) and nominal voltage (V) of battery, respectively, and  $I$  is the battery current (A). Thus, the heat generated by the battery is expressed by Eq. 3

$$Q_{gen} = I(E - v) + T\Delta S \frac{1}{nF}. \tag{3}$$

2.1.2. Cylindrical lithium-ion battery

A 42110 cylindrical LiFePO<sub>4</sub> battery was used, and covered with liquid-cooled cylinder (LCC) as shown in Fig. 2. A cooling channel, liquid-cooled aluminum cylinder with a thickness of 3 mm was installed in the 45 °C

battery. The implemented convergence criteria are 10<sup>-3</sup> for hydrodynamics and 10<sup>-6</sup> for energy. The numbers of mini channels inside LCC considered in this paper are 2, 4, 6, 8, 10, and 12. They were made of aluminum. Water was used as cooling medium with the water flowing from the inlet at the top of battery.

The thermo-physical properties for LCC, battery, and water used in this research are summarized in Table 2 [2]. In this work, heat generation is determined by the following Eq. 4:

$$q_g = -T\Delta S \frac{1}{nF} + I(E - V), \tag{4}$$

where  $T$  denotes the temperature (K) of battery cell,  $I$  is the discharge current (A) of battery cell,  $F$  is the Faraday constant (94.85 C·mol<sup>-1</sup>),  $n$  represents the number of electrons transferred in the electrochemical reaction,  $\Delta S$  is the entropy change (J mol<sup>-1</sup> K<sup>-1</sup>),  $E$  is open circuit voltage (V) and  $V$  is operating voltage (V) [12]. Then, the value of heat generation rate can be determined by using the following Eq. 5:

$$\dot{q}_{generation} = \frac{q_g}{Volume}. \tag{5}$$

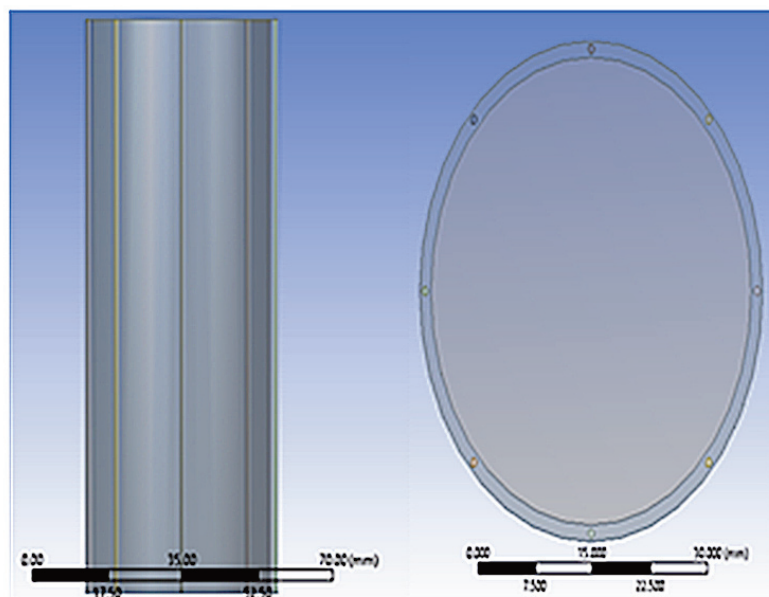


**Fig. 2.** Cylindrical battery with LCC geometry design.

**Table 2.** Thermo-physical properties of LCC, battery, and water

Material	$\rho$ (kg/m <sup>3</sup> )	$c_p$ (J/kg <sup>-1</sup> K <sup>-1</sup> )	$k$ (W/mK <sup>-1</sup> )
Batteries	2450	1108	3.917
Aluminum	2719	871	202.4
Water	998.2	4128	0.6

## 2.2. Numerical solution

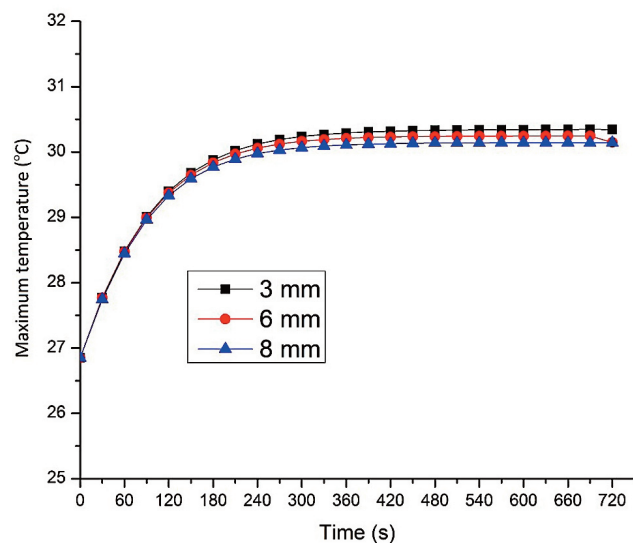
The numerical solution of this study was based on computational fluid dynamics (CFD) that was used to analyze heat transfer and fluid flow in battery cooling system. The first stage was to do meshing by dividing geometry into small element of volume control for the mathematical calculation. A tetrahedral mesh type was used as the main mesh construction. After the meshing process, boundary conditions were determined. Inlet mass flow rates and outflows were selected as inlet and outlet boundary conditions. The outer wall of the battery cell was set as free convection boundary condition with a heat transfer coefficient of 5 W/m<sup>2</sup>K<sup>-1</sup>.

## 3. RESULTS AND DISCUSSION

### 3.1. Physical problem

#### 3.1.1. Prismatic lithium ion battery

The simulation results demonstrate that varying the channel width affects the maximum temperature. For 3 mm

**Fig. 3.** Cell battery temperature graph with mass flow rate  $10^{-3}$  kg/s<sup>-1</sup> under different channel widths.

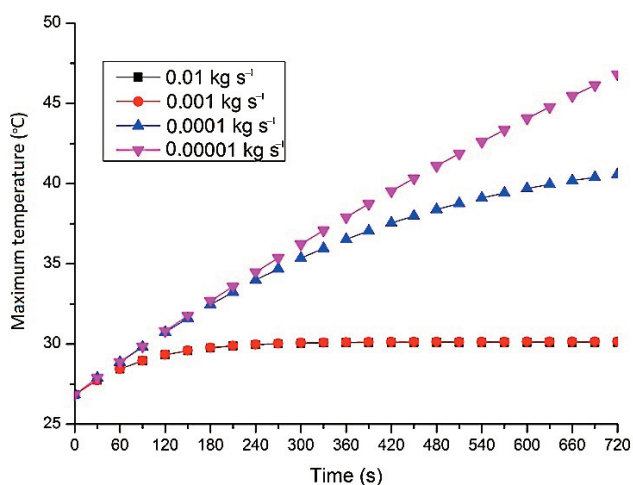
channel it was 30.35 °C, which is 0.1 °C higher than the maximum temperature for 6 mm channel width and 0.12 °C higher than for 8 mm channel width. More detailed results are presented in Fig. 3. Thus, wider channel variations can lower the temperature of battery cells and water flow rates; however, the decrease is not significant when compared to the variations in water flow rate of the water mass.

#### 3.1.2. Effect of mass flow rate

The inlet mass flow rate of  $10^{-4}$  kg/s<sup>-1</sup> increases the maximum battery temperature almost equaling it to the battery operating temperature of 40 °C. The same also occurs when the inlet mass flow rate is less than  $10^{-4}$  kg/s<sup>-1</sup> with the maximum battery temperature rising above 40 °C.

Figure 4 shows that decreasing the inlet mass flow rate increases the battery maximum temperature. When the inlet mass flow rate is  $10^{-3}$  kg/s<sup>-1</sup>, the maximum battery temperature drops almost 10 °C from the battery operating temperature and stabilizes at 29 °C to 30 °C.

The simulation results show that the increase of mass flow rate has an effect on decreasing the maximum battery temperature. According to the theory of heat transfer, the water mass flow rate is not obviously related to the decrease in the temperature of the battery cell, but rather the mass flow rate is influenced by vector flow rate, surface area and fluid density. The flow velocity is closely related to the value of the Reynolds number and Nusselt number. The heat transfer convection coefficient ( $h$ ) is affected by the thermal conductivity ( $k$ ) of water and hydraulic diameter. In this case, the fluid mass flow rate influences the convection coefficient of fluid heat transfer and will ultimately affect the value of heat transfer ( $Q$ ) and cooling performance. Lower cell temperature is

**Fig. 4.** Cell battery temperature graph with channel width 8 mm under different mass flow rates.

observed for the inlet mass flow rate of  $10^{-3}$  kg/s<sup>-1</sup> compared to the inlet mass flow rate of  $10^{-4}$  kg/s<sup>-1</sup> and  $10^{-5}$  kg/s<sup>-1</sup> as shown in Fig. 5a–c. Therefore, the increase of the inlet mass flow rate leads to maximum cooling performance.

Although the inlet of  $10^{-3}$  kg/s<sup>-1</sup> mass flow rate is the best in improving cooling performance compared to the other two variations, there is one more factor to consider in determining the inlet of the water mass flow rate. Both water mass flow rate and pressure drop depend on  $V$ , which is the ratio of mass flow rate (kg/s<sup>-1</sup>) to fluid density ( $\rho$ ), so that large water mass flow rate will affect pumping power as shown in Table 3. The larger channel width lowers the pressure and reduces the energy consumption of the battery cooling system. Hence, the cooling performance can be increased, but with a small pressure drop and minor energy consumption.

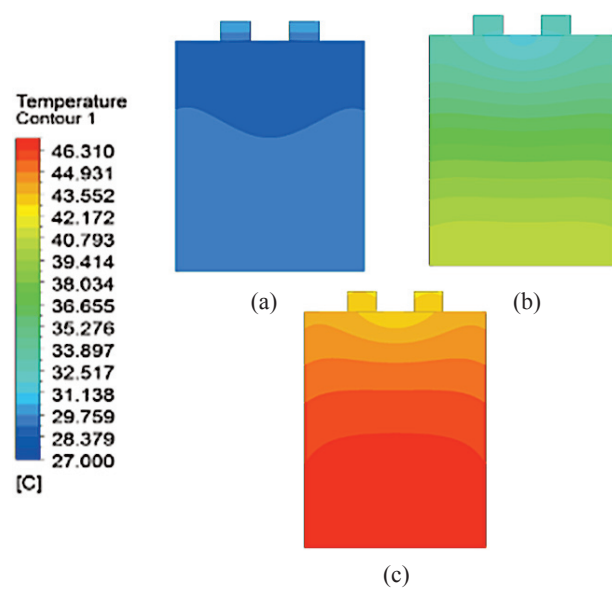


Fig. 5. Cell temperature contour under different mass flow rates: (a)  $10^{-3}$  kg/s<sup>-1</sup>, (b)  $10^{-4}$  kg/s<sup>-1</sup>, (c)  $10^{-5}$  kg/s<sup>-1</sup>.

### 3.2. Cylindrical lithium-ion battery

#### 3.2.1. Effect of channel quality

The temperature and pressure contours of six mini channel variations were compared in this study in order to investigate the effectiveness of cooling performance. The mini channels in cooling systems were distributed evenly in LCC and the mass flow rate of each channel was set to 0.001 kg/s<sup>-1</sup>.

Figure 6 illustrates better cooling performance for higher cooling channel numbers, which maintained the operating temperature below 45 °C. The maximum battery temperature in each cooling channel variation was always measured in the center of the battery as that is the part where the electrode is located. Figure 7 shows considerable decrease in the battery temperature according to simulation results using the CFD compared to the maximum operating temperature of the battery. The highest battery temperature was 35.54 °C with two cooling channels, which cannot be deemed acceptable. Whereas, the batteries with four, six and eight cooling channels had a maximum operating temperature of 34.01 °C, 33.35 °C, and 32.94 °C, respectively. Therefore it is evident that the maximum temperature value in the battery will decrease as the number of channels in the cold plate is increased, because the heat transfer area is expanded due to more channels involved. However, the increasing number of channels does not necessarily cause a significant decrease in the maximum temperature of the battery, as demonstrated in Fig. 7. For both 10 and 12 channels the temperature reduction is 0.2 °C.

Simulation results show that with increasing the number of cooling channels the pressure drop will be smaller. By increasing the number of cooling mini channels the pressure drops are: about 6626 Pa with two mini channels, 2997 Pa with four mini channels, 1936 Pa with six, 1429 Pa with eight, 1137 Pa with 10, and 943 Pa with 12 mini channels cooling. This corresponds to the theory stating that the pressure is inversely proportional

Table 3. Pressure drop and flow velocity value under different mass flow rates and channel widths

No.	Mass flow rate (kg/s <sup>-1</sup> )	Channel width (mm)	Pressure drop (Pa)	Flow velocity (m/s <sup>-1</sup> )
1	$10^{-3}$	3	1539.60	0.67
	$10^{-3}$	6	597.40	0.33
	$10^{-3}$	8	415.53	0.25
2	$10^{-4}$	3	109.50	0.067
	$10^{-4}$	6	49.26	0.033
	$10^{-4}$	8	36.07	0.025
3	$10^{-5}$	3	10.22	0.0067
	$10^{-5}$	6	4.76	0.0033
	$10^{-5}$	8	3.50	0.0025



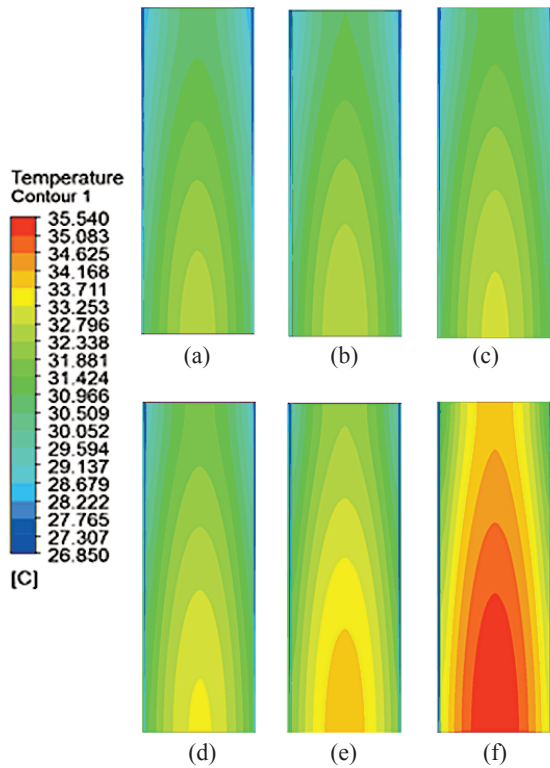


**Fig. 6.** Temperature distribution in battery cell with different number of cooling channels: (a) 12, (b) 10, (c) eight, (d) six, (e) four, (f) two channels.

to the area; by increasing the number of cooling channels the larger the area will be so that the pressure on the channels will decrease. Thus, for the following study, the version with eight channels was selected as the most efficient cooling solution.

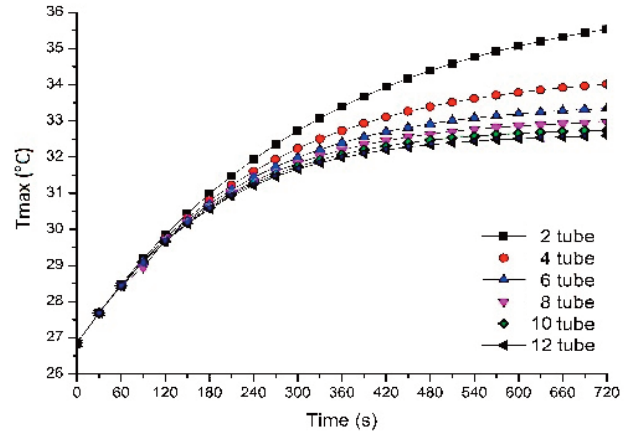


**Fig. 7.** Maximum temperature in battery cell with different number of cooling channels.

### 3.2.2. Effect of mass flow rate

Based on the eight channel LCC cooling system, mass flow rate variations were studied in this section to investigate their effect on the cooling performance. The results are demonstrated in Fig. 8. The graph of mass flow rate variation to maximum temperature in battery is shown in Fig. 9.

The maximum temperature of the battery with a mass flow rate of  $0.00001 \text{ kg/s}^{-1}$  reached  $43.67 \text{ }^\circ\text{C}$ , close to the maximum working temperature of the battery,  $45 \text{ }^\circ\text{C}$ . The faster the flowing fluid, the higher the heat transfer rate will be due to fluid velocity directly affecting the Reynolds number and the Nusselt number. However, higher mass flow rate will raise pressure drop and require more energy to be consumed. Thus, it may not be necessary to use a higher mass flow rate.

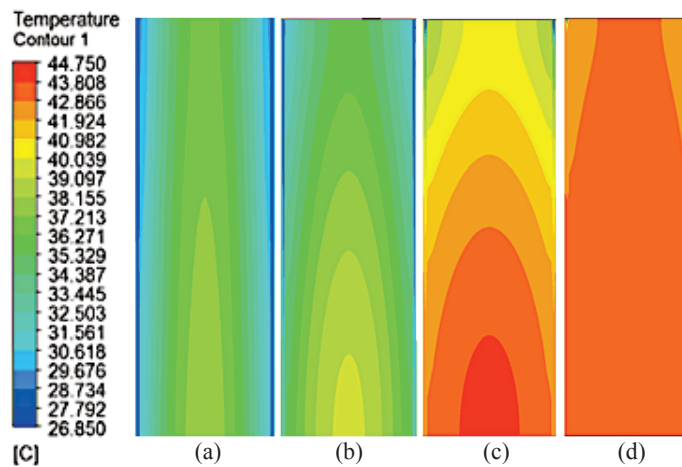


**Fig. 8.** Temperature distribution for mass flow rate: (a)  $0.01 \text{ kg/s}^{-1}$ , (b)  $0.001 \text{ kg/s}^{-1}$ , (c)  $0.0001 \text{ kg/s}^{-1}$ , (d)  $0.00001 \text{ kg/s}^{-1}$ .

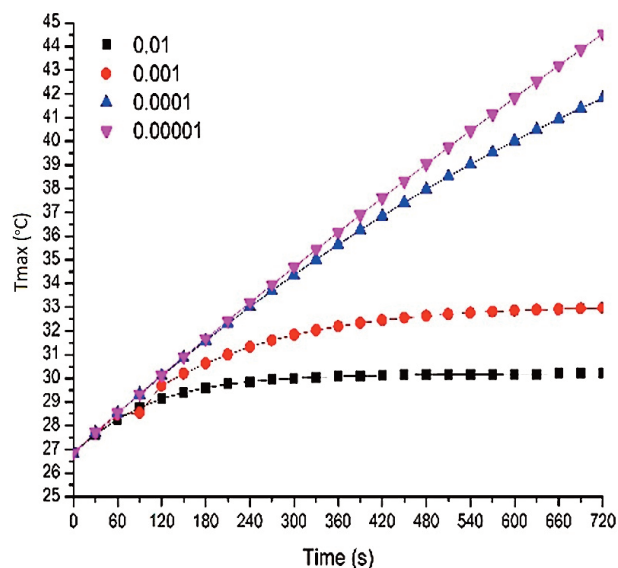


Fig. 9. Maximum temperature under different inlet mass flow rate.

The highest velocity of fluid flowing in the cooling channels reached  $3.862 \text{ m/s}^{-1}$  at a mass flow rate of  $0.01 \text{ kg/s}^{-1}$ . However, at a mass flow rate of  $0.01 \text{ kg/s}^{-1}$  the pressure drop in the channels was very high – at  $20\,575 \text{ Pa}$ . At a mass flow rate of  $0.001 \text{ kg/s}^{-1}$  the fluid velocity within the channels reached  $0.478 \text{ m/s}^{-1}$  with a pressure drop value at  $1429.775 \text{ Pa}$ . At a flow rate of  $0.0001 \text{ kg/s}^{-1}$ , the maximum velocity of fluid flowing in the channels was  $0.048 \text{ m/s}^{-1}$  with pressure drop  $139.465 \text{ Pa}$  and at a mass flow rate of  $0.0001 \text{ kg/s}^{-1}$  the value of fluid velocity flowing in the cooling channels decreased to  $0.005 \text{ m/s}^{-1}$  by the pressure drop value of  $13.493 \text{ Pa}$ . So, the mass flow rate of  $0.001 \text{ kg/s}^{-1}$  was chosen as the most effective mass flow rate for the following study.

In addition to elongating the life cycle, battery management systems will also support the effort for energy efficiency, as these can be adjusted to minimize the dissipation losses. Energy is reflected as valuable asset because it is greatly needed at every time and place [14]. Thus, in a broader sense, battery management systems promotes the circular economy program.

## CONCLUSIONS

To investigate the thermal performance of cylindrical LIB cell, a type of liquid cooling based on liquid-cooled mini channels was used in this study. The influence of channel geometry and mass flow rate were studied. The maximum temperature of the LIB cell can be minimized by increasing the inlet mass flow rate. Increased inlet mass flow rate from  $1 \times 10^{-5} \text{ kg/s}^{-1}$  to  $1 \times 10^{-3} \text{ kg/s}^{-1}$  kept the battery cell maximum temperature down from  $45 \text{ }^\circ\text{C}$  to

$30 \text{ }^\circ\text{C}$ . Although an increase of inlet water mass flow rate was considered as an efficient method, the increase in mass flow rate exceeding  $1 \times 10^{-3} \text{ kg/s}^{-1}$  did not have a major impact on the decrease in the battery cell temperature and increased energy consumption instead. Changes in channel width from  $3 \text{ mm}$  to  $8 \text{ mm}$  can only lower the maximum battery cell temperature by an average of  $0.11 \text{ }^\circ\text{C}$ . Increasing the mass water flow rate is an effective method for lowering the maximum temperature of a lithium-ion battery cell, but it must be balanced by widening the channel of the cooling plate to reduce pressure drop and reduce energy consumption in the battery cooling system. The configuration with eight cooling channels was chosen as the most effective cooling channel version in this case. Increasing the number of cooling channels will reduce the maximum temperature in the battery up to  $12.06 \text{ }^\circ\text{C}$  and about  $0.2 \text{ }^\circ\text{C}$  when the number of channels exceeds eight. Increasing the number of mini channels used will create a more complicated cooling system and raise the cost of fabrication. The mass flow rate of  $0.001 \text{ kg/s}^{-1}$  was considered to be the most efficient. Meanwhile at  $0.001 \text{ kg/s}^{-1}$  the pressure drop value was  $1429.775 \text{ Pa}$  and the amount of pressure drop can affect the required energy consumption. This study helps increasing energy efficiency, which further promotes the circular economy program.

## ACKNOWLEDGEMENT

The publication costs of this article were covered by the Estonian Academy of Sciences.

## REFERENCES

1. Rao, Z. and Wang, S. A review of power battery thermal energy management. *Renew. Sust. Energ. Rev.*, 2011, **15**(9), 4554–4571.
2. Qian, Z., Li, Y. and Rao, Z. Thermal performance of lithium-ion battery thermal management system by using mini-channel cooling. *Energy Convers. Manag.*, 2016, **126**, 622–631.
3. Mahamud, R. and Park, C. Reciprocating air flow for Li-ion battery thermal management to improve temperature uniformity. *J. Power Sources*, 2011, **196**(13), 5685–5696.
4. Azizi, Y. and Sadrameli, S. M. Thermal management of a LiFePO<sub>4</sub> battery pack at high temperature environment using a composite of phase change materials and aluminum wire mesh plates. *Energy Convers. Manag.*, 2016, **128**, 294–302.
5. Hamidah, N. L., Nugroho, G., Wang, F. M. Electrochemical analysis of electrolyte additive effect on ionic diffusion for high-performance lithium ion battery. *Ionics*, 2016, **22**, 33–41.
6. Hamidah, N. L., Nugroho, G., Wang, F. M. The understanding of solid electrolyte interface (SEI) formation and

- mechanism as the effect of fluoro-o-phenylenedimaleimide (F-MI) additive on lithium-ion battery. *Surf. Interface Anal.*, 2019, **51**, 345–352.
7. Greco, A., Cao, D., Jiang, X. and Yang, H. A theoretical and computational study of lithium-ion battery thermal management for electric vehicles using heat pipes. *J. Power Sources*, 2014, **257**, 344–355.
  8. Xu, J., Lan, C., Qiao, Y. and Ma, Y. Prevent thermal runaway of lithium-ion batteries with minichannel cooling. *Appl. Therm. Eng.*, 2017, **110**, 883–890.
  9. Lan, C., Xu, J., Qiao, Y. and Ma, Y. Thermal management for high power lithium-ion battery by minichannel aluminum tubes. *Appl. Therm. Eng.*, 2016, **101**, 284–292.
  10. Fan, L., Khodadadi, J. and Pesaran, A. A parametric study on thermal management of an air-cooled lithium-ion battery module for plug-in hybrid electric vehicles. *J. Power Sources*, 2013, **238**, 301–312.
  11. Chen, D., Jiang, J., Kim, G., Yang, C. and Pesaran, A. Comparison of different cooling methods for lithium-ion battery cells. *Appl. Therm. Eng.*, 2016, **94**, 846–854.
  12. Zhao, J., Rao, Z. and Li, Y. Thermal performance of mini-channel liquid cooled cylinder based battery thermal management for cylindrical lithium-ion power battery. *Energy Convers. Manag.*, 2015, **103**, 157–165.
  13. Huo, Y., Rao, Z., Liu, X. and Zhao, J. Investigation of power battery thermal management by using mini-channel cold plate. *Energy Convers. Manag.*, 2015, **89**, 387–395.
  14. Makijenko, J., Burlakovs, J., Brizga, J. and Klavins, M. Energy efficiency and behavioral patterns in Latvia. *Manag. Environ. Qual.*, 2016, **27**(6), 695–707.

### Silindrilise liitiumioonaku termilise jõudluse uurimine

Thalita Maysha Herninda, Laurien Merinda, Ghina Kifayah Putri, Enda Grimonia,  
Nur Laila Hamidah, Gunawan Nugroho, Erkata Yandri, Ivar Zekker, Idrees Khan,  
Luqman Ali Shah ja Roy Hendroko Setyobudi

Silindrilise liitiumioonaku elemendi termilise jõudluse uurimiseks kasutati selles töös vedeljahutusega minikanaleid. Uuriti kanalite geomeetria ja massivoolukiiruse mõju liitiumaku jahutusele, kuna jahutuse probleem on üks olulisemaid aku kõrgel koormusel kasutamisel eettulevaid probleeme. Liitiumioonaku elemendi maksimaalset temperatuuri saab minimeerida, suurendades vedeliku sisselaskeava massivoolu kiirust. Sisselaskeava massivoolukiiruse suurendamine tasemelt  $1 \times 10^{-5} \text{ kg/s}^{-1}$  tasemele  $1 \times 10^{-3} \text{ kg/s}^{-1}$  alandas akuelemendi maksimaalse temperatuuri  $45 \text{ }^\circ\text{C}$ -lt  $30 \text{ }^\circ\text{C}$ -ni. Kuigi sisendvee massivooluhulga suurendamist peeti tõhusaks meetodiks, ei avaldanud massivoolukiiruse suurenemine üle  $1 \times 10^{-3} \text{ kg/s}^{-1}$  olulist mõju akuelemendi temperatuuri langusele ja energiatarbimise võimekuse suurenemisele. Vedeljahutuse kanali laiuse muutus  $3 \text{ mm}$ -lt  $8 \text{ mm}$ -le võib akuelemendi maksimaalset temperatuuri langetada ainult keskmiselt  $0,11 \text{ }^\circ\text{C}$  võrra. Vee massivoolukiiruse suurendamine on tõhus meetod liitiumioonaku elemendi maksimaalse temperatuuri alandamiseks, kuid seda tuleb tasakaalustada jahutuskanali laiendamisega, et vähendada rõhu langust ja energiakulu aku jahutussüsteemis. Leiti, et tõhusaim jahutuskanalite arv on kaheksa. Mida rohkem minikanaleid kasutatakse, seda enam tõstab jahutussüsteemide lisamine aku tootmiskulusid.